Chapter 5

HIGH TEMPERATURE PROPERTIES OF ($Al_3Zr+ZrB_2$)/Al-Mg HYBRID COMPOSITE

5.1 Introduction

In order to check the suitability of ($Al_3Zr+ZrB_2$)/Al-Mg composite for high temperature applications, tensile and dry sliding wear tests were conducted at different temperatures starting from room temperature to 250°C at an interval of 50°. Tests were carried out on Al-Mg base alloy and C3 composite (i.e. with 10 vol.% Al_3Zr + 3 vol.% ZrB_2).

5.2 Tensile Properties

The engineering stress-strain curves of base alloy and hybrid ($Al_3Zr+ZrB_2$)/Al-Mg *insitu* composite are shown in Fig. 5.1 at different temperature from 50°C to 250°C at an interval of 50°. It is observed that ambient temperature ultimate tensile strength (UTS), yield strength (YS) and percentage elongation are improved in the hybrid composite as compared to Al-Mg alloy. But with increase in test temperature, above properties show a decreasing trend in hybrid composite. The tensile properties have been evaluated from the engineering stress-strain curves for all test temperatures and the variation of these properties with temperature is shown in Fig. 5.2, which clearly indicates that the values of UTS, YS and percentage elongation decrease with increase in temperature.

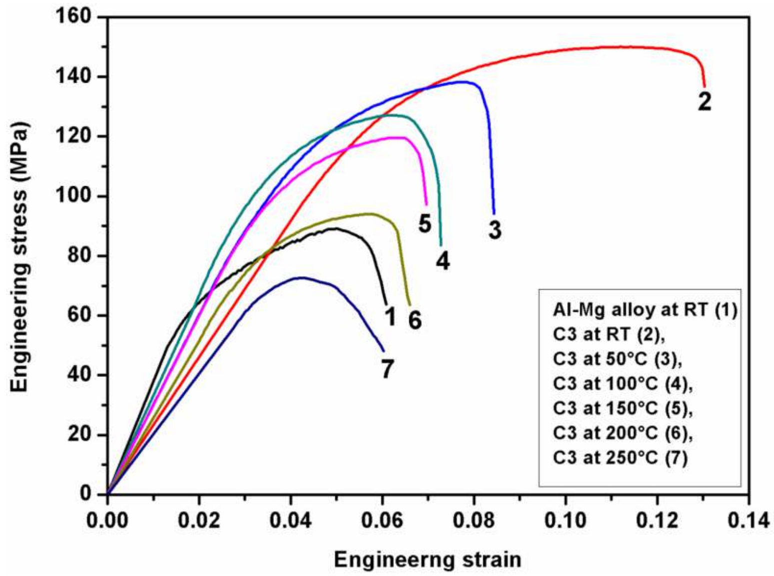

Figure 5.1 – Engineering stress-strain curves of the Al-Mg alloy and hybrid composite at different temperatures.

The improvement in room temperature strength parameters of hybrid composite as compared to base alloy is due to the presence of second phase reinforcement particles in the alloy matrix. These hard particles refine the aluminium grains and act as barrier in the motion of dislocation in the composite, hence, cause the strength parameters to improve [Zhang et al., 2007; and Tian et al., 2014]. The improvement in elongation of hybrid composite as compared to matrix alloy may be attributed to grain refinement, because these refined grains retard the growth and propagation of crack during tensile loading [Tian et al., 2014].

Figure 5.2 shows the variation of UTS with temperature in hybrid composite. It is clear that the UTS decreases with increase in test temperature, but the effect of temperature on UTS up to 150°C in hybrid composite is not significant, and the reduction in UTS is only about 20% up to 150ºC. Hybrid composite consists of hard reinforcement particles which are stable up to this temperature and impede the dislocation during tensile test. But above this temperature, the values of Ultimate tensile strength reduce sharply which may be due to the coarsening of grains. Yield strength also exhibits similar kind of behavior with test temperature. Figure 5.2 also shows the variation of percentage elongation with increasing temperature in hybrid composite. It shows that the percentage elongation decreases continuously with an increase in test temperature. The reduction in elongation or ductility may be due to the nucleation of inter-granular cracks and segregation of second phase hard particles in the grain boundary region during deformation process at elevated temperature.

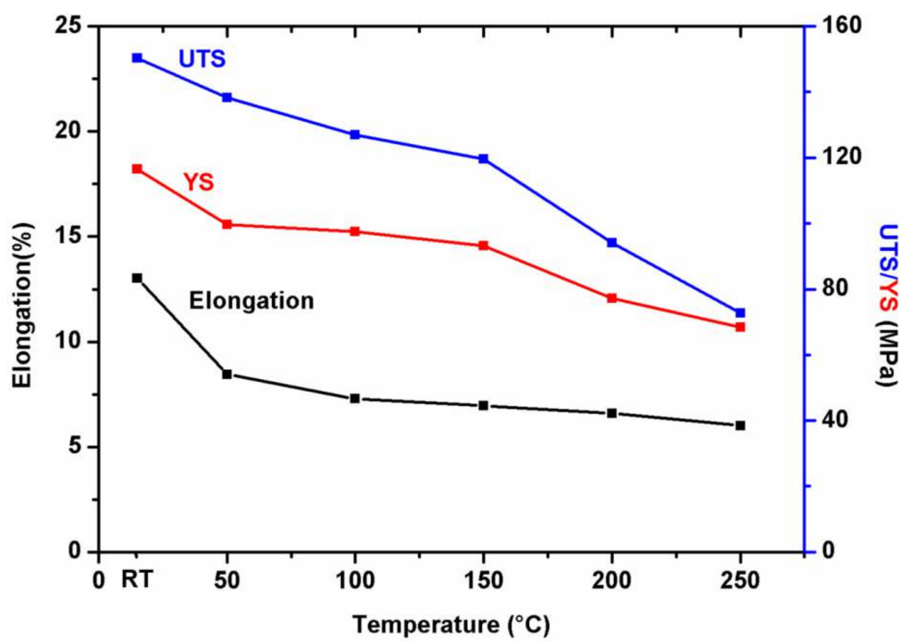

Figure 5.2 – Variation of mechanical properties in composite with temperatures.

To understand the effect of temperature on the flow curve properties of hybrid composite, the strain hardening exponent (n) and strength coefficient (K) have been evaluated with the help of Fig. 5.3 which shows the log-log plot of true stress (σ) versus true strain (ε_p) with test temperature under constant strain rate of 1.07 $\times 10^{-3}$ s^{-1}. It is observed that the flow stress, slope between true stress and true strain and intercept on the true stress decrease with increasing test temperatures. Strain hardening exponent (n) and strength coefficient (K) have been plotted in Fig. 5.4. From this figure it is observed that the values of strain hardening exponent (n) and strength coefficient (k) decrease continuously with an increase in test temperature. With increase in test temperature, rate of work hardening reduces due to thermal softening of materials which leads to decrease in the values of n and K. There is rapid decrease in the values of n and K beyond 150°C which may be due to debonding of ZrB_2 reinforcement particles which leads to crack generation and propagation.

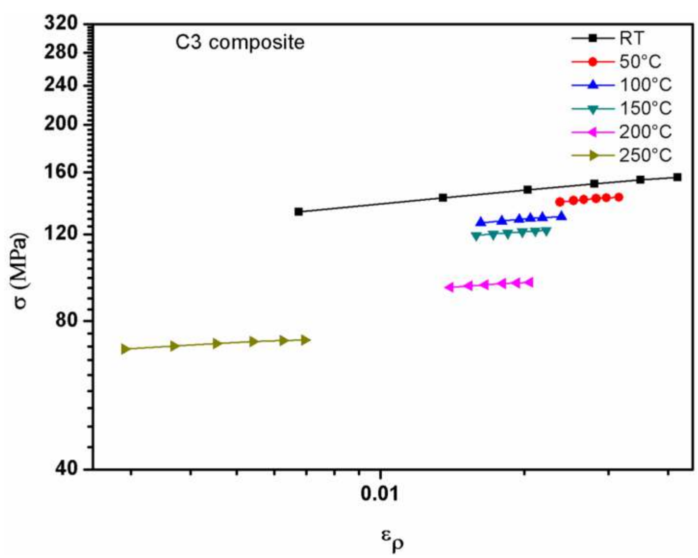

Figure 5.3 – σ vs. ε_ρ plots of hybrid composite with temperatures on log-log scale.

Figure 5.5 shows the scanning electron micrographs of tensile fractured surface of hybrid composite at different test temperatures. At room temperature, the mode of fracture is quasi cleavage showing the presence of dimples and flat regions (Fig. 5.5a). Similar mode of fracture is observed with different size void formation due to the debonding of ZrB_2 clusters and crack in Al_3Zr particles at few places, when the composite sample is tested at 100°C (Fig. 5.5b). But at 250°C, the fractured surface shows the brittle cleavage mode of fracture with plastic deformation in some regions (Fig. 5.5c). This kind of brittle behaviour can be attributed to the relative weakness of the grain boundary. These results are also in agreement with the tensile results of hybrid composite at different temperatures (Fig. 5.2). The summarized data of mechanical properties of the composite for different temperatures is given in Table 5.1.

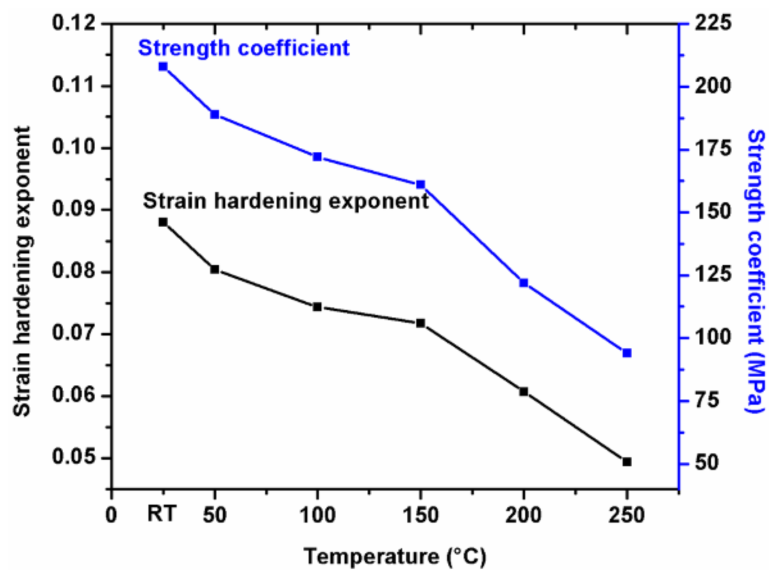

Figure 5.4 – Variation of flow curve properties in composites with temperatures.

5.3 Tribological Properties

5.3.1 Effect of Temperature

Figure 5.6 shows the variation of wear rate and coefficient of friction with test temperature at an interval of 50° for constant sliding velocity, sliding distance and normal load for Al-Mg alloy and hybrid composite. It is seen from Fig. 5.6a that for Al-Mg alloy wear rate decreases initially followed by a sharp increase with increase in test temperature. But for hybrid composite wear rate increases initially with increasing temperature and then decreases with further increase in temperature and finally it increases rapidly for the temperature beyond 150°C. But still wear rate is lower than the wear rate of Al-Mg alloy at 250°C. However, coefficient of friction increases continuously with test temperatures for Al-Mg alloy and hybrid composite (Fig. 5.6b).

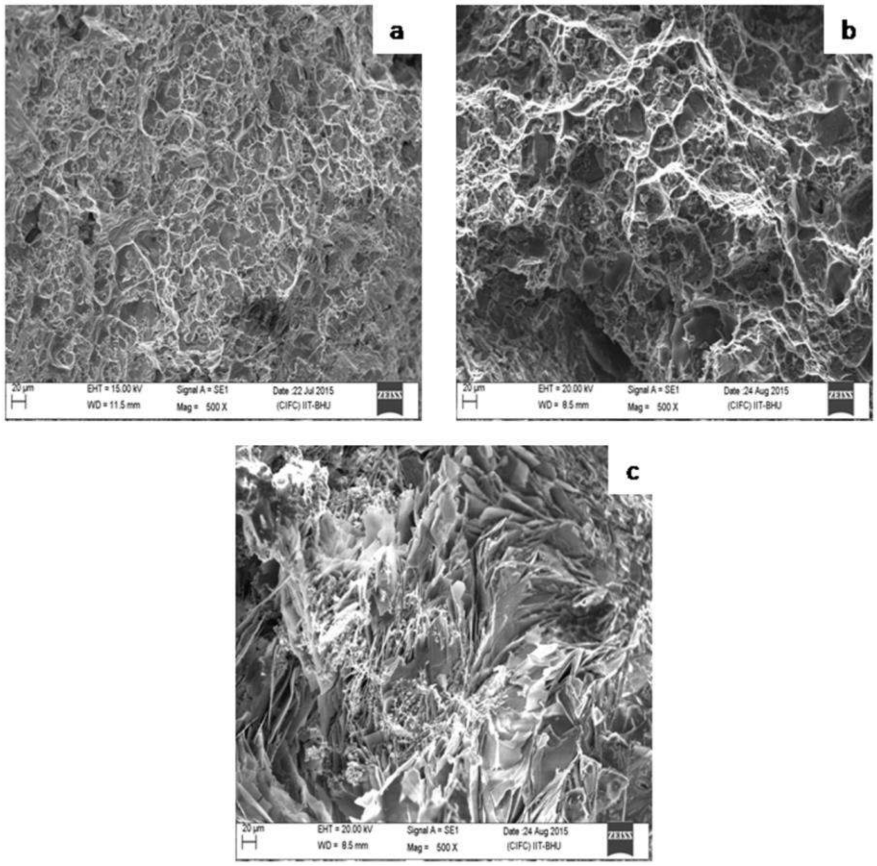

Figure 5.5 – Scanning electron microstructures of tensile fracture surface of composite at different temperatures (a) room temperature, (b) 100°C and (c) 250°C.

Table 5.1 – Summarized data of mechanical properties of composite for different temperatures.

Composite	**Temperature (°C)**	**Strength (MPa)**		**Elongation (%)**	**Flow curve parameters**	
		UTS	**YS**		**Strain hardening exponent, n**	**Strength coefficient, K (MPa)**
C3	RT	150.3	116.5	13.01	0.08800	208
	50	138.2	99.7	8.45	0.08041	189
	100	127.0	97.5	7.28	0.07430	172
	150	119.6	93.2	6.96	0.07169	161
	200	94.0	77.2	6.59	0.06068	122
	250	72.7	68.4	6.01	0.04938	94

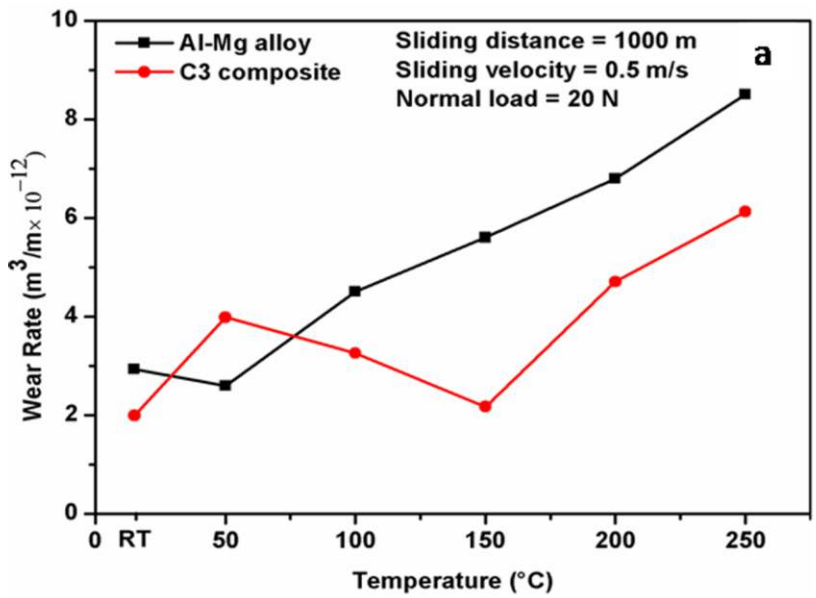

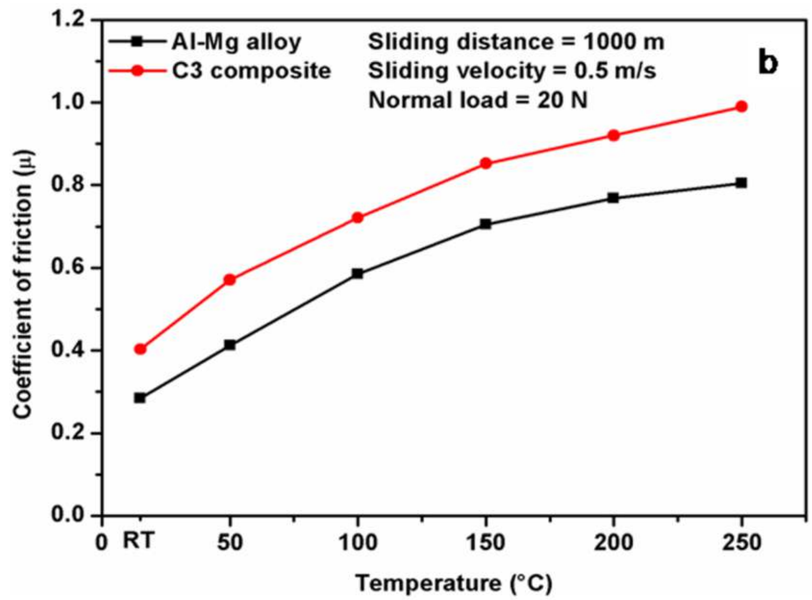

Figure 5.6 – Effect of temperature on (a) wear rate, and (b) coefficient of friction at constant sliding distance, sliding velocity and load.

5.3.2 Effect of Load

Figure 5.7 shows the variation of wear rate and coefficient of friction with normal load at constant sliding velocity, sliding distance and test temperature for Al-Mg alloy and hybrid composite. It is seen that wear rate increases with increasing normal load (Fig.

5.7a), while coefficient of friction shows a completely reverse trend and it decreases with normal load for both Al-Mg alloy and hybrid composite (Fig. 5.7b).

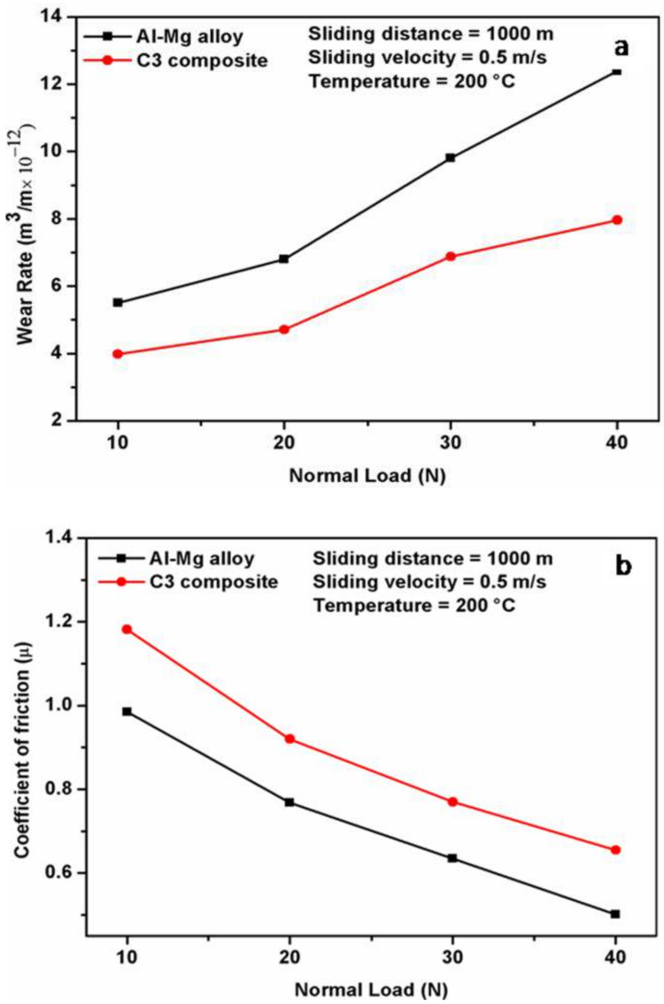

Figure 5.7 – Effect of normal load on (a) wear rate, and (b) coefficient of friction at constant sliding distance, sliding velocity and temperature.

5.3.3 Effect of Composition

Figure 5.8 shows the variation of wear rate and coefficient of friction with composition at constant sliding velocity, sliding distance and load. It is seen that wear rate decreases in case of hybrid composite as compared to Al-Mg alloy for all temperatures except 50°C (Fig. 5.8a). However, coefficient of friction increases for hybrid composite as compared to Al-Mg alloy for all temperatures (Fig. 5.8b).

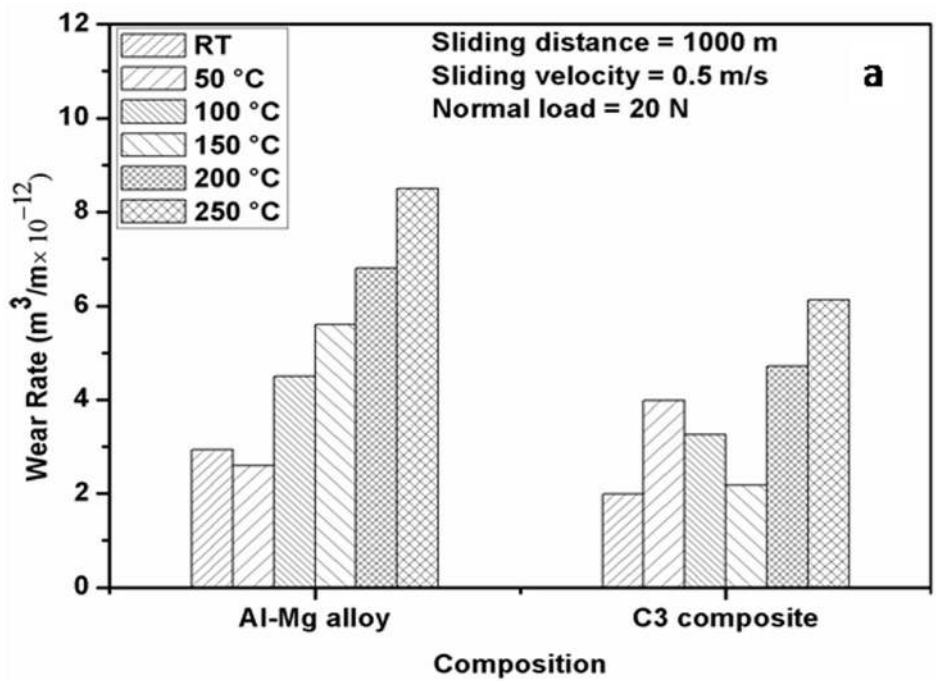

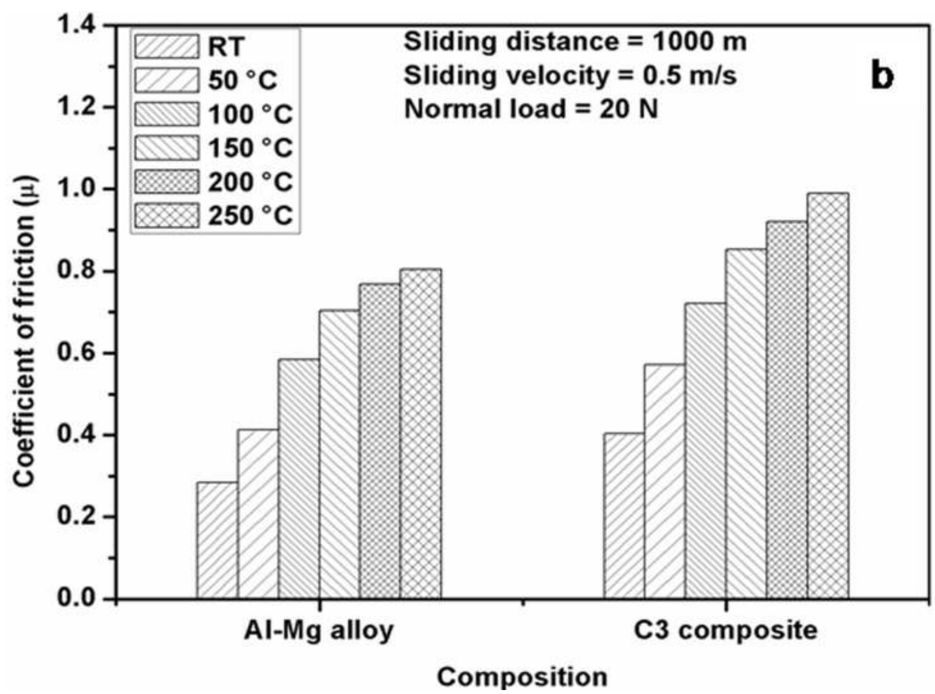

Figure 5.8 – Effect of composition on (a) wear rate, and (b) coefficient of friction with constant sliding distance, speed and normal load at different temperatures.

5.3.4 Worn Surface Studies and Mechanism

There are two important categories of parameters influencing wear and friction properties namely operating parameters (i.e. applied load, sliding velocity, temperature and test duration) and structural parameter (i.e. materials in contact and their properties).

Wear test has been carried out on Al-Mg alloy and hybrid composite consisting of ZrB_2 particles (3 vol.%) and Al_3Zr particles (10 vol.%) at different loads (10 to 40 N) and test temperatures (room temperature to 250°C) for constant sliding speed and distance. The test could not be continued beyond 250°C temperature because of excessive surface damage and gross material transfer.

Figure 5.6a shows the variation of wear rate with test temperature. Aluminium base matrix is prone to oxidation even at room temperature, and rate of oxidation is likely to increase with rise in temperature. In the present case wear rate of Al-Mg alloy initially decreases with increasing temperature due to the formation of oxide layer, but with further increase in temperature, wear rate increases due the breakage or removal of the thick oxide layer on continuous sliding. While in hybrid composite wear and friction are likely to depend on large Al_3Zr particles and clusters of fine ZrB_2 particles. With increase in temperature softening of matrix takes place and larger particles protrude from the surface. These particles may be removed due to pressure, thereby increasing the wear rate. But with further increase in temperature and softening of matrix these protuberances merge with the matrix. Rate of oxidation increases and the oxide layer covers the contact surface causing wear rate to decrease (Fig. 5.9a-b). As the temperature is further raised beyond 150°C, thick oxide layer breaks and soft matrix is unable to hold the hard particles. SEM of worn surface reveal severe delamination of surface and large amount of metal flow leading to deep grooves (Fig. 5.9c-d). As a result, wear rate of hybrid composite increases sharply (Fig. 5.6a).

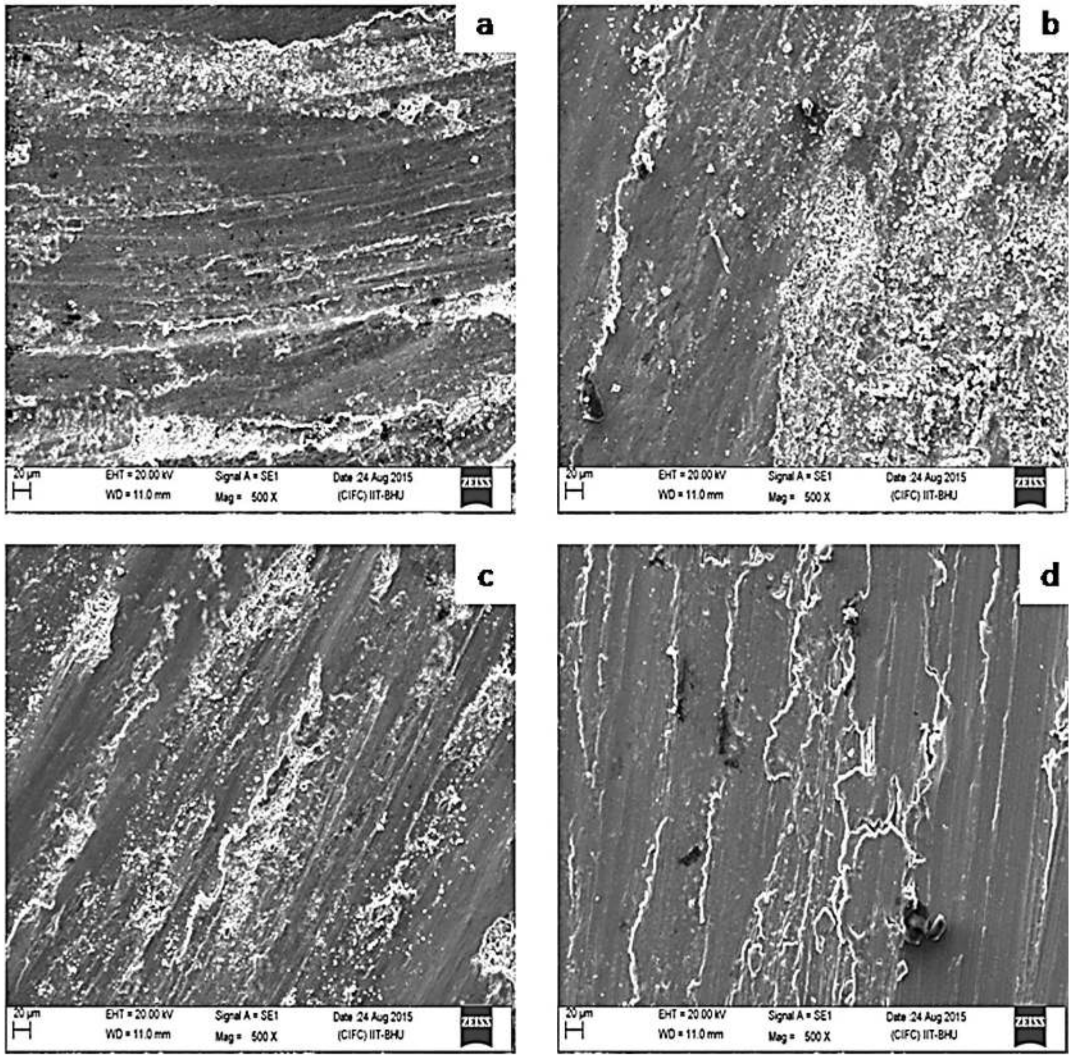

Figure 5.9 – Scanning electron microstructures of worn surfaces of hybrid composite at constant sliding speed 0.5 m/s and normal load of 40 N for different temperatures (a) 100°C, (b) 150°C, (c) 200°C, and (d) 250°C.

SEM study of wear debris in Fig. 5.10 shows the presence of large flakes. Hard particles act as protuberances with softening of surface and formation of excessive oxide with increase in temperature increase the coefficient of friction continuously (Fig. 5.6b). Further, profilometer results are also in agreement (Fig. 5.11a-b) and surface roughness values of 4.00 and 8.64 μm are observed at 100°C and 250°C respectively.

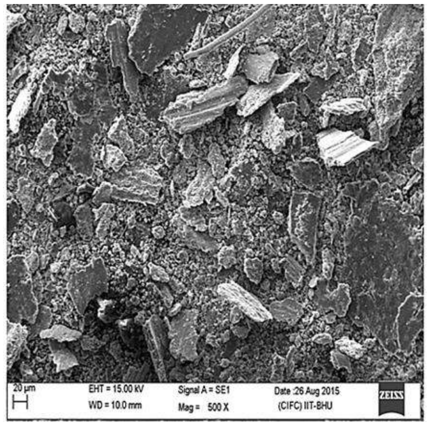

Figure 5.10 – Scanning electron microstructure of wear debris in hybrid composite at 250°C.

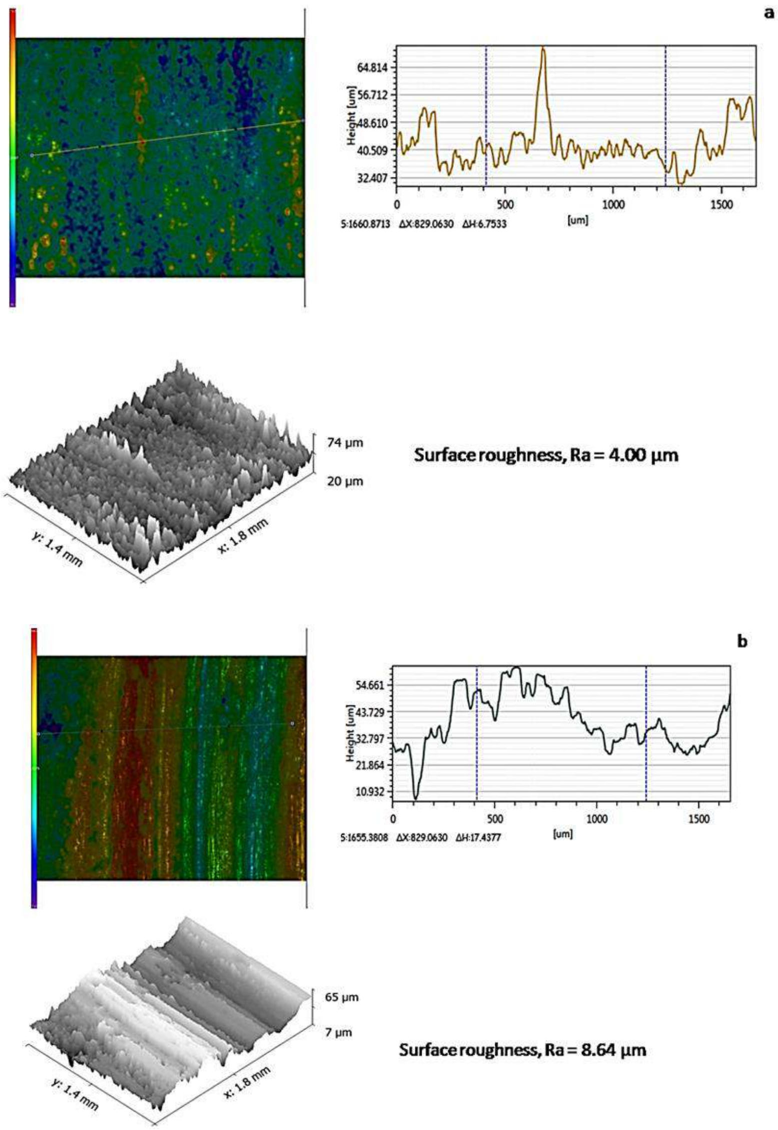

Figure 5.11 – Height analysis perpendicular to worn surface and its 3D-profilometric images with the value of surface roughness at constant sliding speed 0.5 m/s and the normal load of 40 N at different temperature (a) 100°C, and (b) 250°C.

Delamination increases and surface gets highly deformed as the load increases. The roughness values are found to be 3.90 to 7.11 μm at 20 N and 40 N loads respectively (Figs. 5.12 & 5.13). Wear rate increases continuously (Fig. 5.7a), whereas, coefficient of friction shows a decreasing trend with load. COF may decrease due to the softening of base alloy which keeps the hard particles merged within itself, or it may allow hard particles to flow away and coefficient of friction is reduced (Fig. 5.7b).

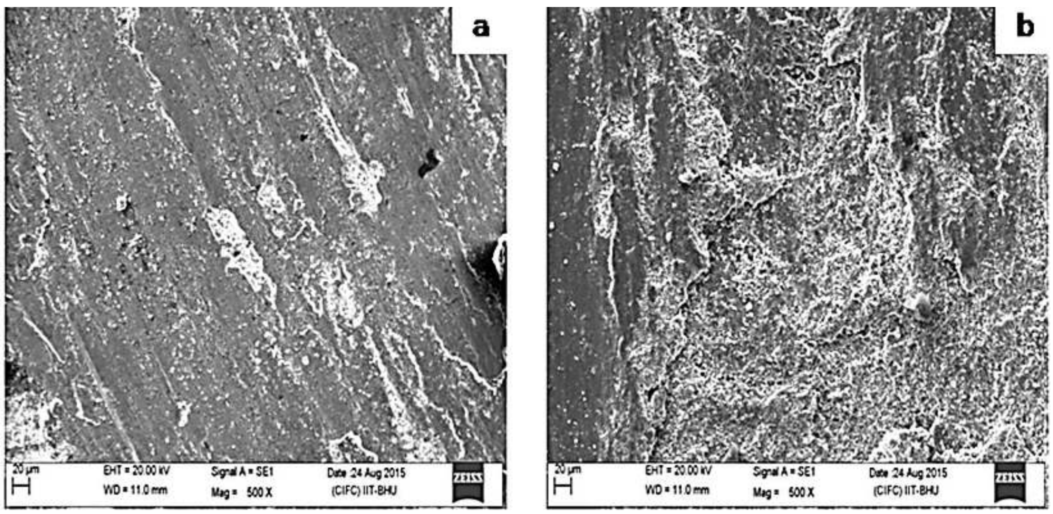

Figure 5.12 – Scanning electron microstructures of worn surfaces of hybrid composite at constant sliding speed 0.5 m/s and temperature of 200°C for different normal load (a) 20 N, and (b) 40 N.

It has already been observed (cf; Ch. 3 & 4) that with *insitu* formation of hard Al_3Zr and ZrB_2 particles in Al-Mg alloy, refinement of Al-rich grains takes place and presence of hard second phase particles generates dislocations in the Al-rich matrix. Overall situation leads to improvement in strength and hardness of the composite and wear rate is reduced as compared to Al-Mg alloy at room temperature. Even at high temperature, composites are likely to have higher hardness and strength that helps to restrict wear rate of composite at lower value as compared to Al-Mg alloy.

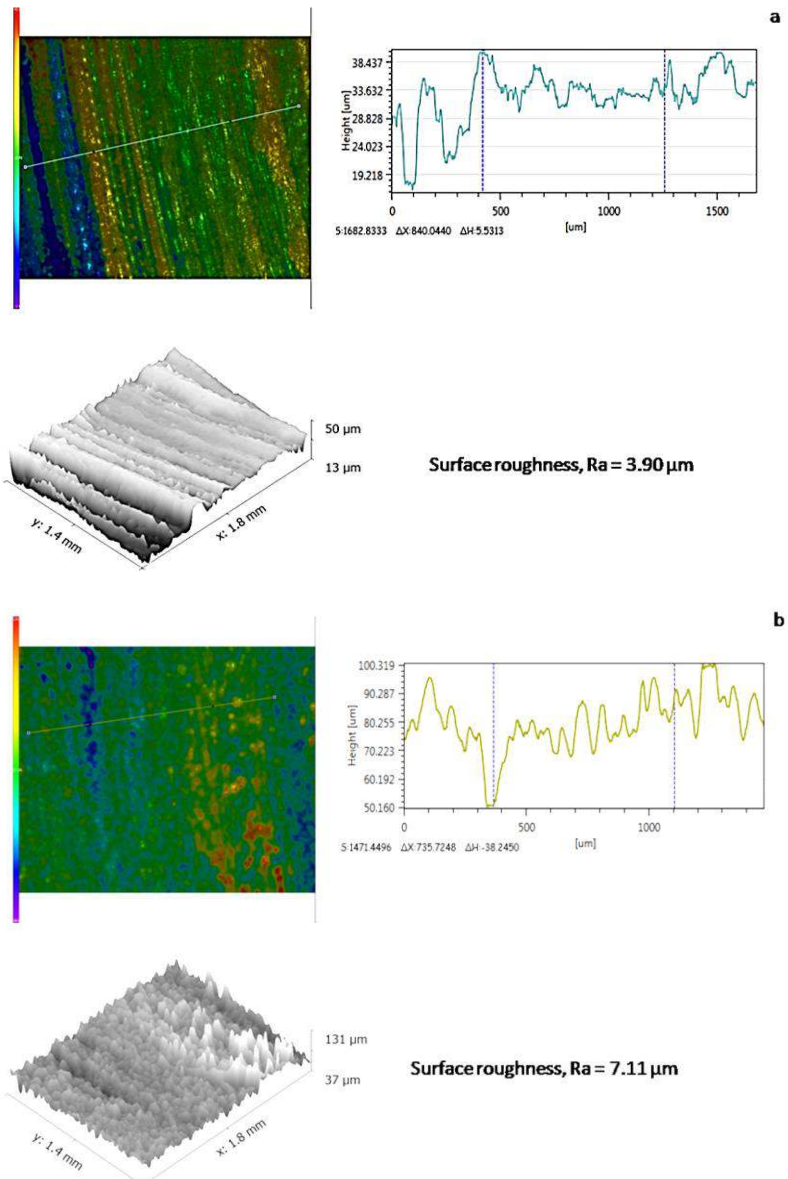

Figure 5.13 – Height analysis perpendicular to worn surface and their 3D-profilometric images with the surface roughness value at constant sliding speed 0.5 m/s and temperature 200°C for different normal loads (a) 20 N, and (b) 40 N.

Improvement in strength restricts the delamination of the surface during test. As a result89 of these, the wear rate of composite decreases as compared to Al-Mg alloy and the minimum wear rate is observed at 150 °C (Fig. 5.8a). The profilometer results are also in agreement (Fig. 5.14a-b). The roughness values decrease from 4.61 to 2.51 µm with the incorporation of hard particles in Al-Mg alloy for the wear test conducted at 150 °C. Further, the coefficient of friction improves with incorporation of hard particles in the Al-Mg alloy. COF is contribution of large number of factor (adhesion, ploughing, deformation and third body) but in the present case the particle contribution (i.e. third body) to friction is more as compared to other factors which increases the overall coefficient of friction.

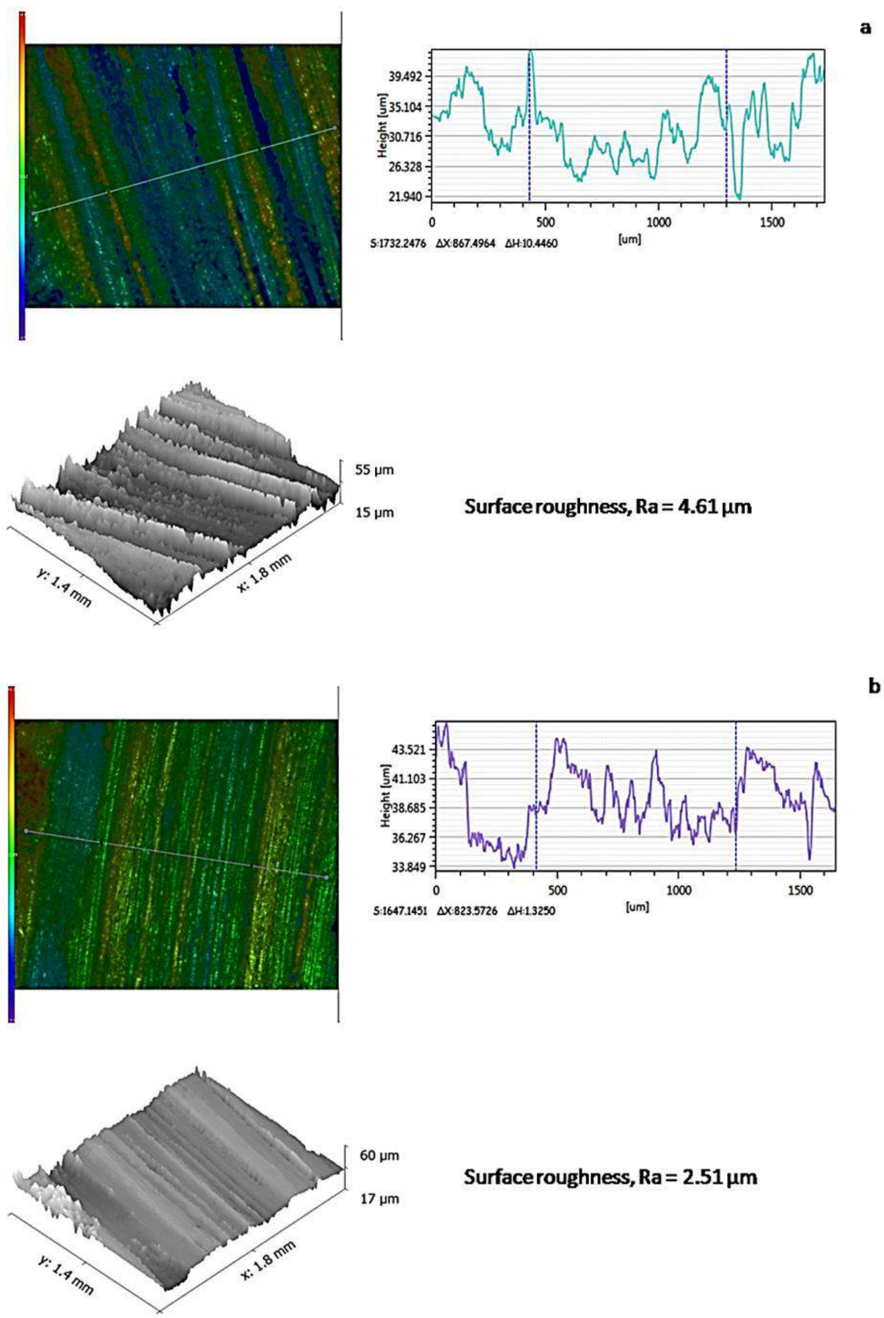

Figure 5.14 – Height analysis perpendicular to worn surface and its 3D-profilometric images with the value of surface roughness at constant sliding speed 0.5 m/s and temperature 150°C of (a) Al-Mg alloy, and (b) hybrid composite.

5.4 Conclusions

On the basis of present study following conclusions have been drawn:

1. Ultimate tensile strength, yield strength and percentage elongation decrease with increase in test temperature.
2. The values of strain hardening exponent (n) and strength coefficient (K) decrease continuously with increase in test temperature.
3. The fractography of hybrid composite shows a quasi-cleavage (mixed) mode of fracture up to 100°C but at high temperature i.e 250°C the cleavage mode of fracture with plastic deformation is identified.
4. In Al-Mg alloy wear rate decreases initially followed by a sharp increase with increase in test temperature, however, in hybrid composite after an initial increase wear rate decreases with increase in temperature but above 150°C wear rate increases rapidly though it remains lower than the wear rate of Al-Mg alloy even at 250°C.
5. Coefficient of friction increases continuously with test temperature.
6. Wear and friction results indicate that the wear rate increases with increase in normal load, whereas coefficient of friction shows a decreasing trend.
7. The transition of mild to severe wear is shifted to higher temperature with incorporation of Al_3Zr and ZrB_2 particles in the Al-Mg alloy.
8. Mild/oxidative and severe/oxidative-metallic wear is observed at different combinations of parameters.
9. SEM and profilometer results are in agreement with wear and friction results.